JOURNAL OF Applied Polymer SCIENCE

Comparison of Morphology and Mechanical Properties of Peroxide-Cured Acrylonitrile Butadiene Rubber/LDH Composites Prepared from Different Organically Modified LDHs

Jianxiang Feng,[1,2] Zedong Liao,[1] Jin Zhu,[2] Shengpei Su[1]

[1]Key Laboratory of Sustainable Resources Processing and Advanced Materials of Hunan Province, Department of Chemistry and Chemical Engineering, Hunan Normal University, Changsha, Hunan 410081, China

[2]Polymers and Composites Division, Ningbo Institute of Material Technology and Engineering Chinese Academy of Science, Ningbo, Zhejiang 315201, China

Correspondence to: S. Su (E-mail: sushengpei@gmail.com)

ABSTRACT: Rubber compounds based on acrylonitrile butadiene rubber (NBR) containing organically modified layered double hydroxides (LDHs) were prepared using peroxide as a curing agent. The LDHs intercalated by organic compounds including sodium styrene sulfonate (SSS) and sodium dodecylbenzene sulfonate (SDBS) were investigated using thermogravimetric analysis (TGA) and X-ray diffraction (XRD) while the unmodified LDHs were used as contrast. Experimental results from TGA and XRD showed that both SSS- and SDBS-intercalated LDHs were successfully obtained. The morphology of the LDH composites was characterized by scanning electron microscopy (SEM), transmission electron microscopy (TEM), and XRD. The chemical structure of NBR/LDHs compounds were measured by Fourier transform infrared spectrum. The thermal properties were measured by TGA and differential scanning calorimetry. Other properties such as mechanical and swelling properties were also investigated. The results showed that a chemical bonding between organically modified LDHs and rubber matrix through SSS was built during vulcanization, which leads to improved interfacial strength of the cured compound. A high-performance acrylonitrile butadiene rubber/SSS-modified LDH compound, which has two times higher tensile strength than cured pure rubber without significant loss of elongation, was obtained.
 J. Appl. Polym. Sci. 000: 000–000, 2012

KEYWORDS: acrylonitrile butadiene rubber; layered double hydroxides; mechanical properties; morphology; dispersion

Received 26 September 2010; accepted 20 March 2012; published online
DOI: 10.1002/app.37746

INTRODUCTION

Layered double hydroxides (LDHs)-filled polymer composites have attracted a lot of interest both from academia and industry because of their improved properties in thermal stability,[1,2] flammability,[1,3,4] mechanical properties,[5] and gas barrier property[6] when compared with their virgin polymers. This enhancement in properties is mainly due to the effective dispersion of LDH layers within the polymer matrix. However, LDHs as fillers of composites belong to anionic clays of high charge density, small gallery height, and strong hydrophilicity. They consist of layers of divalent (M^{2+}) and trivalent (M^{3+}) cations coordinated octahedrally by hydroxyl groups with a structure similar to that of brucite, $Mg(OH)_2$, in which isomorphous replacement of the divalent cation with trivalent cation creates a positive charge on the metal layers which is counter balanced by the presence of anions in the galleries.[7] These anions could be ion exchanged like cations in cationic clays. In general, to obtain good dispersion of LDHs in a hydrophobic polymer matrix, the pristine LDHs have to be modified with organic anions, and many kinds of anions have been successfully intercalated into LDHs, including the common inorganic anions, carboxylates, organosulfates, polymeric anions, and complex anions such as polyoxometalate.[8,9] Several methods including coprecipitation, anion exchange, calcination, and rehydration have been studied to obtain organically modified LDH, and various thermoplastic and thermosetting polymers including poly(methyl methacrylate),[10,11] polystyrene,[11,12] polyamide 6,[13,14] poly(vinyl chloride),[15] epoxy,[16,17] and polyethylene[5,18–21] have been reported as matrixes to prepare LDH composites. In contrast, investigations have only very recently started on rubber/LDH composites such as composites of ethylene vinyl acetate,[22–26] ethylene propylene diene monomer rubber,[27] carboxylated nitrile,[28] chloroprene

Table I. Compound Formulation of NBR/LDH Composites

Sample	NBR (phr)	DCP (phr)	SSS-LDH (phr)	SDBS-LDH (phr)	LDH-NO_3 (phr)
NBR	100	1	-	-	-
NBR-L	100	1	-	-	3
NBR-SL	100	1	5	-	-
NBR-SDL	100	1	-	5	-

phr: parts per hundred rubber.

rubber,[29,30] and natural rubber.[30] However, to the best of our knowledge, there are only few reactive organically modified LDHs, which could chemically react with rubbers under the curing condition, have been used to prepare rubber/LDH composites.[31]

In this work, sodium styrene sulfonate (SSS) will be used as a reactive organic modifier; this organically modified LDH together with pristine LDH and sodium dodecylbenzene sulfonate (SDBS)-modified LDH will be used to prepare NBR/LDH composites using peroxide curing system. It is expected that the reactive double bond of SSS will enhance the interface interaction between NBR and LDH in peroxide curing process and will result in composites with excellent properties.

EXPERIMENTAL

Materials

Acrylonitrile butadiene rubber (NBR; N41, acrylonitrile content 29%) was obtained from China Petrochemical Corporation (Lanzhou, China). Dicumyl peroxide (DCP) was supplied by Shanghai Shanpu Chemical Reagent (Shanghai, China). Magnesium nitrate ($Mg(NO_3)_2{\cdot}6H_2O$) and aluminum nitrate ($Al(NO_3)_3{\cdot}9H_2O$) were purchased from Xinjida Chemical Company (Taiyuan, China). SSS was purchased from Zichuan Yaodong Chemical (Zibo, China). Sodium hydroxide (NaOH) and SDBS were supplied by Sinopharm Chemical Reagent (Shanghai, China). All the materials were used without further purification.

Preparation of Mg–Al LDH

Mg–Al LDH was synthesized by coprecipitation method, following a procedure similar to that reported by Meyn et al.[32] The preparation was carried out in an N_2 atmosphere, and the distilled water used in the preparation was boiled for 30 min and cooled to room temperature under N_2 atmosphere before use to exclude CO_2 whose presence would lead to the incorporation of carbonate in the LDHs. A solution containing Al^{3+} and Mg^{2+} with a Mg^{2+} : Al^{3+} molar ratio of 3 was prepared by dissolving $Mg(NO_3)_2{\cdot}6H_2O$ (15.4 g) and $Al(NO_3)_3{\cdot}9H_2O$ (7.5 g) in 80 mL of deionized water. This solution was slowly dropped into 20 mL of vigorously stirred decarbonated water, while a solution of 2*M* of NaOH was added simultaneously to maintain pH of the reaction mixture at 10 ± 0.5. After the addition of the nitrate solution, the resulting precipitate was aged at 80°C for 24 h under N_2 atmosphere with continuous stirring and was then filtered. The sample was washed several times with decarbonated water until nitrate free (Brown Ring Test was used to test the nitrate) and dried at 80°C in a vacuum oven until the water content in LDH was about 30 ± 2 wt %. All the operations were performed under N_2 atmosphere.

Treatment of LDH by Anionic Surfactants

Ion exchange of SDBS or SSS with LDH-NO_3 was carried out using decarbonated water as a dispersing liquid. A mixture of 6.6 g of the LDH-NO_3 and 200 mL of decarbonated water was stirred at 40°C for 2 h. Then, a solution of 4.1 g of the SSS (or SDBS 6.9 g) in 100 mL of decarbonated water was added dropwise to the LDH dispersion under vigorously stirring. After the addition of anionic surfactant solution, the precipitation was aged for 24 h with stirring. Finally, the resulting white solid was filtered and washed several times with decarbonated water until nitrate free and then dried at 80°C in a vacuum oven. All the operations were performed under N_2 atmosphere.

Preparation of NBR/LDH Composites

Rubber composites were prepared in an open two-roll mill. The compound formulations of NBR/LDH composites are shown in Table I. The LDH loading of each NBR/LDH compound (including LDH-NO_3, SSS-LDH, and SDBS-LDH) was 3 wt %. After NBR and LDH were mixed in an open two-roll mill for 15 min, water was evaporated out and then the crosslinking agent DCP was added. The samples were denoted as NBR-L, NBR-SL, and NBR-SDL for LDH-NO_3-, SSS-LDH-, and SDBS-LDH-filled composites, respectively. Moving-die rheometer was used to obtain curing parameters such as scorch time, optimum cure time, and the graphs of vulcanization. The specimens were cured at 160°C in an electrically heated hydraulic press under a pressure of 10 MPa for 30 min. Dumbbell-shaped specimens of the composites according to GB/T 528-1998 were made by cutting out from the compression-molded sheets of virgin polymers and the composites.

Characterization

Thermogravimetric analysis (TGA) scans were made from 30 to 800°C using a Netzsch STA409 PC instrument (Netzsch, Germany) under a flowing N_2 atmosphere at a scan rate of 10°C/min. All TGA results are the average of a minimum of three determinations; temperature is reproducible to ±3°C, and the error bars on the nonvolatile material is ±3%. X-ray diffraction (XRD) patterns were collected from 1° to 40° and scan time of 10 seconds per step, using a Bruker D8 instrument (Bruker, Germany) with a step size of 1°. Cu Kα X-ray radiation (λ = 0.154 nm) was used and generated at 40 kV. The Fourier transform infrared (FTIR) spectra of the LDHs and NBR composites were obtained using a WQF-200 spectrometer (Rayleigh, China) over a frequency range of 400–4000 cm^{-1}. The powdered samples were mixed with KBr and pressed in the form of pellets for

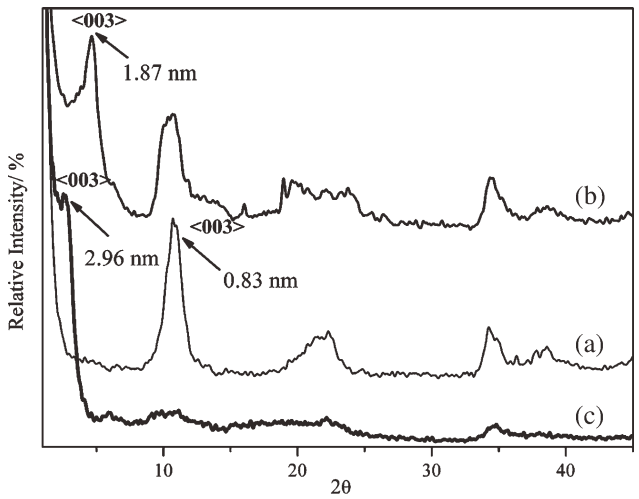

Figure 1. XRD traces obtained from (a) NO_3-LDH, (b) SSS-LDH, and (c) SDBS-LDH.

FTIR analysis. The vulcanization properties were recorded on a moving Die Rheometer (Tianyuan, China). Tensile testing of the NBR samples were carried out using a WDW3020 (Kexin, China) according to the standard GB/T 528-1998 at a strain rate of 500 mm/min at 25°C ± 2°C. Differential scanning calorimeter (DSC) analysis was performed on a TA Q20 series calorimeter (New Castle, PA) from −50 to 10°C under a flowing N_2 atmosphere at a ramp rate of 10°C/ min. The scanning electron microscopy (SEM) was performed on a S-4800 instrument (Hitachi, Japan) to study the fractured surface of the composites. The state of aggregation of the LDH particles in NBR matrix was investigated by microscopy, which was carried out at room temperature using Tecnai F20, transmission electron microscope (TEM) with acceleration voltage (200 kV), and bright field illumination. The ultrathin sections of the samples were prepared by ultramicrotomy (Leica Ultracut UCT) at −100°C with a thickness of about 100 nm. The solvent uptake capacity (xylene, 25°C) and crosslinking density (number of active network chain segments per unit volume) were determined on the basis of rapid solvent-swelling measurement by the application of Flory-Rehner equation.[33]

Table II. Vulcanization Characteristics of NBR/LDH Nanocomposites

	NBR	NBR-L	NBR-SL	NBR-SDL
t_{10} (s)	36	37	39	34
t_{90} (s)	403	351	427	350
M_L (N/m)	1.5	1.4	1.3	1.4
M_H (N/m)	4.5	4.1	4.7	4.4
M_H–M_L (N/m)	3.0	2.7	3.4	3.0

t_{10}: scorch time; t_{90}: cure time to 90% of maximum torque development; M_L: minimum torque; M_H: maximum equilibrium torque; M_H–M_L: increscent of torque.

RESULTS AND DISCUSSION

Characterization of LDH and Organically Modified LDHs

The XRD patterns of the LDHs are shown in Figure 1. It is obvious that all the LDHs are of well-defined layered structure. The *d*-spacings of LDH-NO_3, SSS-LDH, and SDBS-LDH are 0.825, 1.87, and 2.96 nm, respectively. The *d*-spacings of SSS-LDH and SDBS-LDH are increased to 1.05 and 2.14 nm, respectively, when compared with that of LDH-NO_3, indicating that both SSS and SDBS were successfully intercalated into the LDH gallery.[11]

In this research, the thermal stability of different LDHs was also studied using TGA. TGA traces are shown in Figure 2, in which the temperature at 5% loss of weight is taken as the onset degradation temperature ($T_{5\%}$); the temperature at 50% loss of weight is defined as the degradation temperature ($T_{50\%}$). From the thermal degradation trace of NO_3-LDH (Figure 2, peak a), one could see two stages: the first weight loss stage at 190°C, which is due to the loss of physical and interlayer water molecules; and the second stage at 450°C, which is contributed to the conversion of hydroxyl groups of the brucite-like layers into

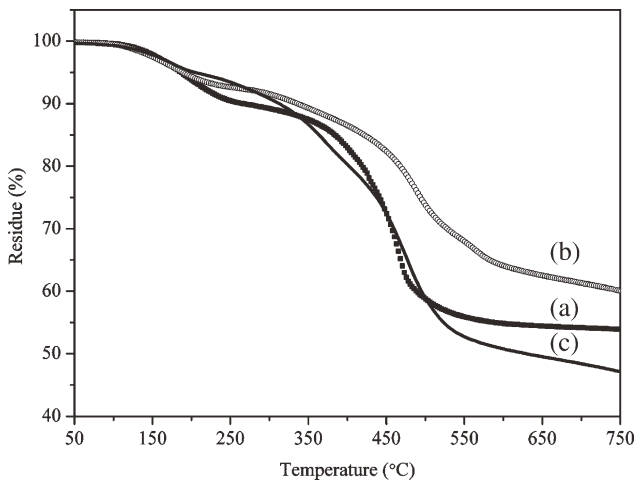

Figure 2. TGA traces obtained from (a) NO_3-LDH, (b) SSS-LDH, and (c) SDBS-LDH.

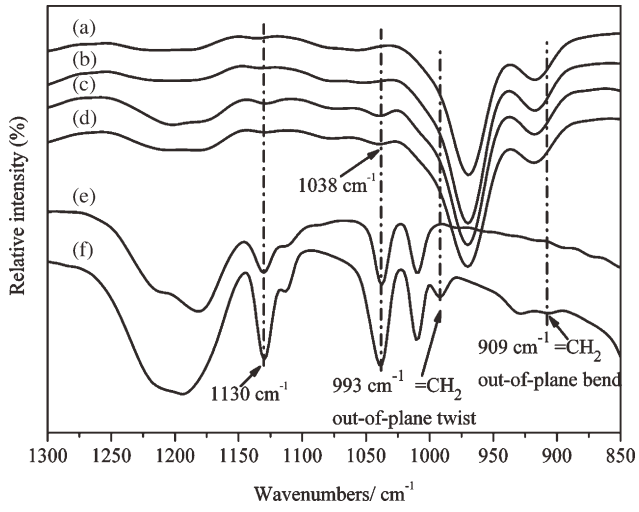

Figure 3. FTIR spectra obtained from (a) NBR, (b) NBR-L, (c) NBR-SL, (d) NBR-SDL, (e) SDBS-LDH, and (f) SSS-LDH.

Table III. Crosslinking Density and Thermodynamical Characteristics of NBR Compounds

Sample	Swelling index	Volume fraction	Crosslinking density (mol/cm^3)	ΔG_m (J/mol)	ΔS [J/(mol K)]
NBR	3.16	0.2953	3.045 E−04	−42.17	1.392 E−01
NBR-L	3.09	0.2978	3.118 E−04	−43.23	1.427 E−01
NBR-SL	2.99	0.3066	3.376 E−04	−47.00	1.551 E−01
NBR-SDL	3.02	0.3033	3.277 E−04	−45.55	1.503 E−01

oxide groups. From the TGA traces of organo-LDHs, one could see three stages: the first weight loss stage at 190°C, more like that of NO_3-LDH; the second stage at 350–360°C, which is because of the thermal degradation of organic modifiers in the interlayer; and data show that SSS-LDH is more stable than SDBS-LDH. It is obvious that, in this region, the degradation of organic anions and the LDHs should be considered.[11] It has been shown that the thermal degradation temperatures of SSS-modified LDH and SDBS-modified LDH have been improved either on 5 wt % weight loss or 10 wt % weight loss. When the 10 wt % weight loss is selected as a comparison point, the decomposition temperature of SSS-modified LDH and SDBS-modified LDH is about 70 and 47°C higher than that of LDH-NO_3.

Vulcanization Property Analysis

As described earlier, three different LDHs are mixed into NBR matrix; the modifiers in LDH are different: for the NBR-L, the filler is LDH-NO_3 without organic modification; for the NBR-SL and NBR-SDL, the fillers are SSS-modified LDH and SDBS-modified LDH, respectively. The difference between SSS and SDBS is that SSS has functional group of carbon–carbon double bond (—HC=CH_2), whereas SDBS has a long hydrophobic chain. The content of LDH in NBR/LDH composites is kept the same, and therefore, we are able to identify how the organic modifiers affect the vulcanization process.

According to Dluzneski,[34] there were three steps in the peroxide curing process. To know the effect of the filler, these three steps need to be clarified. The first step in the crosslinking reaction is the homolytic cleavage of a peroxide molecule to form two free radicals. As the acidic materials can interfere with the homolytic cleavage of peroxide, the basic material is generally recommended. LDH has basic hydroxyl groups on its surface and can act as a basic filler,[28] and therefore, it should not interfere with the homolytic cleavage of peroxide in the first step. This is confirmed by no obvious change of the t_{10} from Table II. The second step is the abstraction of a hydrogen atom from a polymer chain. Interference of this step is that there are some unsaturated sites in a coagent. The mechanism was a combination of self-polymerization as plastic-like reinforcement *in situ* and grafting to polymer chain as a branched structure. The final step of peroxide vulcanization is the coupling of two radicals on adjacent polymer chains to form a crosslinking structure. The t_{90} (427 s) of NBR-SL was the longest among the four materials, which must be resulted from the double carbon bond in SSS. For the existence of the double bond, the polymerization and the grafting reaction of SSS together with the coupling reaction delayed the whole vulcanization process. For the NBR-SDL and NBR-L, the cure time is shorter than that of pure NBR, which may be due to the presence of basic LDH. Because in the first step of the peroxide vulcanization, basic material was favorable for the homolytic cleavage of peroxide, the whole curing time was accelerated. The increasing torque, M_H–M_L, of NBR-SL was much higher than other NBR composites. This result was in good accordance with what is presented in the research of Dluzneski[34] and Henning et al.[35,36] as a result of the addition of vulcanization coagent. This corresponds to the stiffness and crosslinking density results as shown in Tables III and IV.

FTIR Analysis of NBR Composites

FTIR spectra of organically modified LDHs, NBR, and NBR/LDH compounds are shown in Figure 3. For the SSS- and SDBS-modified LDHs, the FTIR spectrum in Figure 3 (peaks e and f) shows the presence of characteristic SO_3 group band at about 1138 and 1050 cm^{-1} for the stretching vibration of SO_3 group.[11] The difference, stemmed from SSS and SDBS chemical structure, between the two organically modified LDHs can also be observed from the FTIR spectra. SSS-LDH exhibits two extra peaks around 993 and 909 cm^{-1}, corresponding to the =CH_2 out-of-plane twist and =CH_2 out-of-plane bend, respectively.

As analyzed before, the double bond of SSS can react during the curing of rubber and lead to the disappearance or decrease of double bond. This is displayed by the FTIR spectrum shown in Figure 3 (peak d). The bands at 993 and 909 cm^{-1} in SSS-LDH were not observed in NBR-SL compound, which confirmed that on vulcanization, some sort of reaction exists between the polymer and the SSS in the layered material.[37]

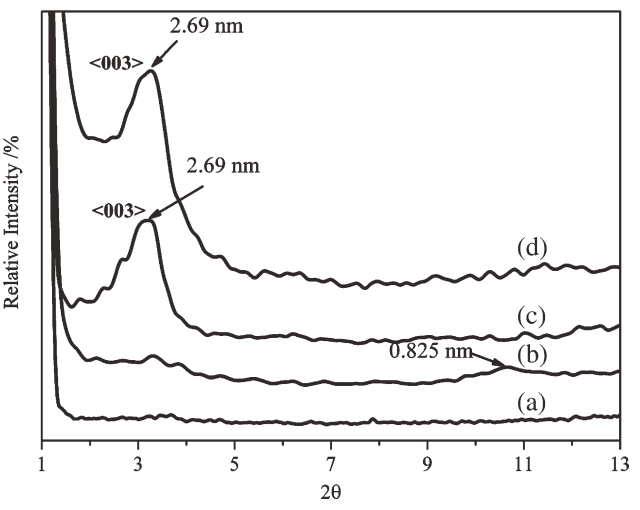

Figure 4. XRD traces obtained from (a) NBR, (b) NBR-L, (c) NBR-SL, and (d) NBR-SDL.

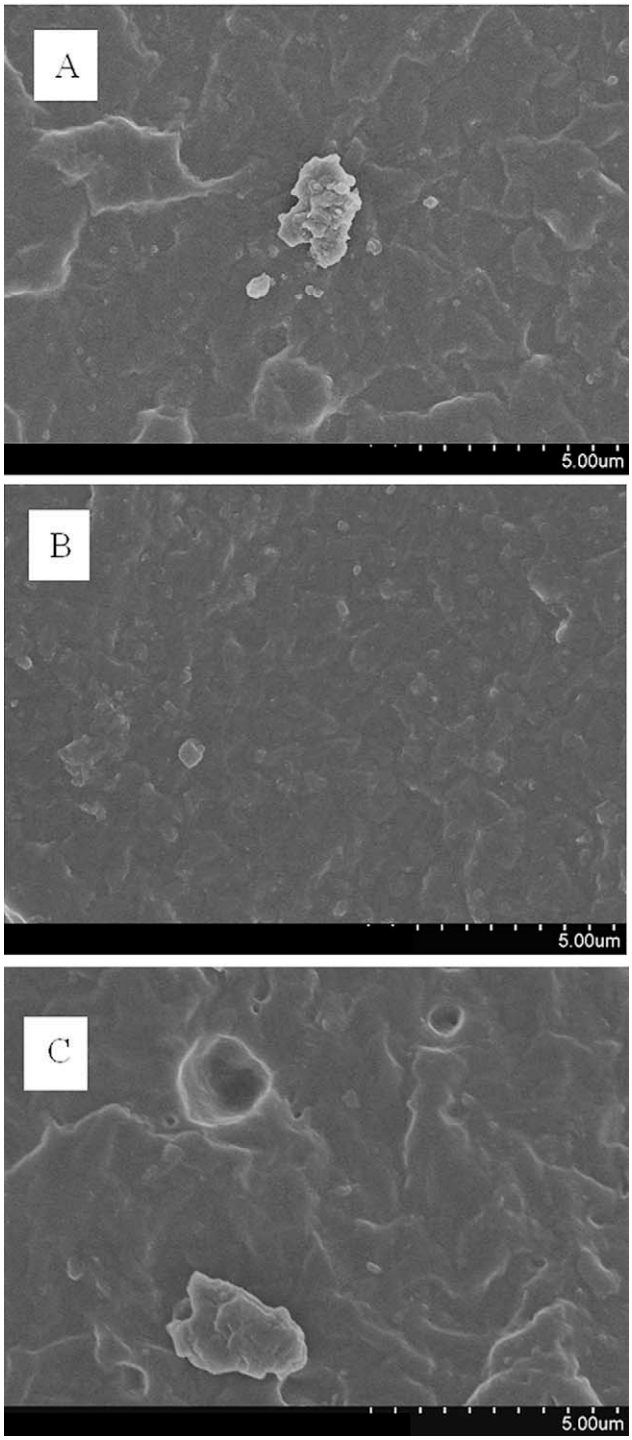

Figure 5. SEM images of (A) NBR-L, (B) NBR-SL, and (C) NBR-SDL at the magnification of 10 000 times.

According to Figure 3 (peaks a and b), there is no obvious peak in 1138 and 1050 cm^{-1} corresponding to S=O structures, which is consistent with the structure of NBR and NBR-L. However, the characteristic peaks of S=O in 1138 and 1050 cm^{-1} is obvious both in NBR-SL and NBR-SDL for filled by SSS-LDH and SDBS-LDH. These differences suggest that on mixing and vulcanization, NBR/LDH composites are successfully obtained.

Swelling Index and Crosslink Density

The effect of the incorporation of the organically modified LDHs on the crosslinking density of NBR can be estimated by the application of the Flory-Rehner equation. The crosslinking density and thermodynamic characteristics of the NBR compounds are shown in Table III. The crosslinking density of

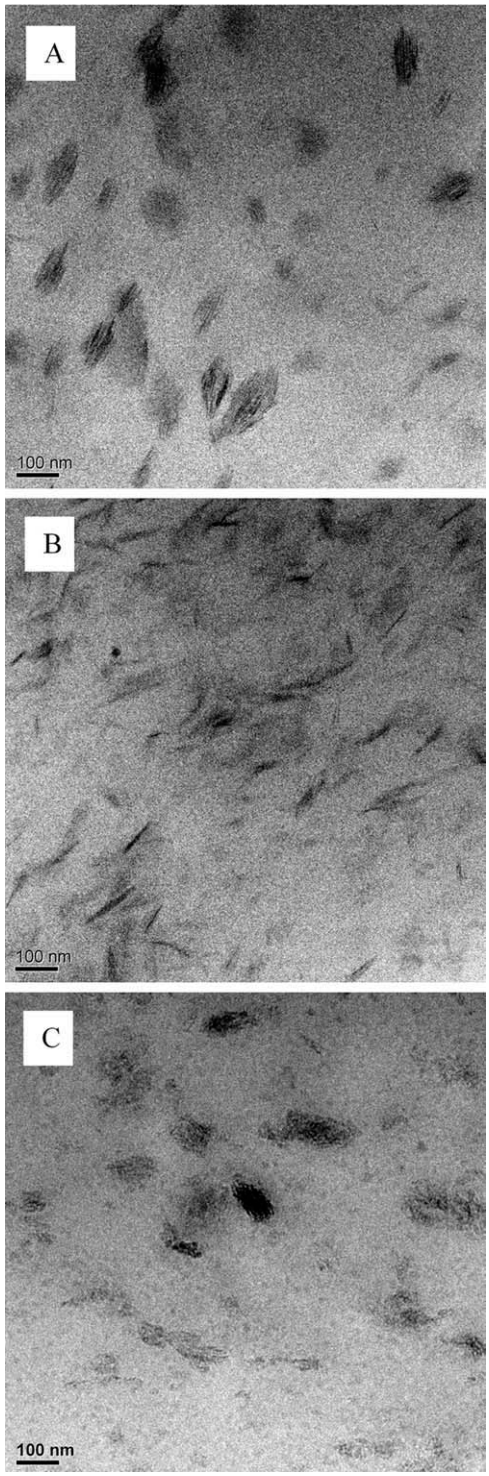

Figure 6. TEM images of (A) NBR-L, (B) NBR-SL, and (C) NBR-SDL (magnification bar: 100 nm).

Table IV. Mechanical Properties of NBR Compounds

Sample	Shore A hardness	Tensile strength (MPa)	Elongation at break (%)	Permanent set (%)
NBR	54	3.1 ± 0.3	279 ± 14	3
NBR-L	56	3.1 ± 0.2	257 ± 14	3
NBR-SL	60	6.7 ± 0.6	261 ± 20	5
NBR-SDL	57	3.6 ± 0.4	268 ± 6	3

NBR-SL is significantly higher than the other NBR composites, which is well consistent with the vulcanization characteristics and the tensile properties discussed above. The results indicate that SSS-modified LDH has strong interaction with the NBR matrix. The thermodynamic parameters, ΔG and ΔS, of the NBR composites are also evidence of strong interaction between SSS-LDH and NBR, which are shown in Table III. A considerable increase in the free energy is observed in the NBR-SL composites. These results can be attributed to better compatibility between the SSS-LDH and NBR matrix so that the NBR molecules can penetrate into the galleries more easily.[38]

XRD Analysis

From XRD measurements, one can either observe a shift and/or broadening or the disappearance of the peak. If a peak is observed shifted to lower values of 2θ, this is typically indicative of intercalation. If the peak does not shift and remains sharp, this likely means that the clay is simply present as an additive without any enlargement of the gallery space. Finally, if the peak vanishes or is significantly broadened, this is indicative of some disordering that could either suggest disordering without insertion of the polymer between the clay layers, a microcomposite, or disordering accompanied by polymer insertion, exfoliation.[39]

The X-ray traces of NBR and NBR/LDH composites are shown in Figure 4. As can be seen from Figure 4 (peak b), the basal spacing (d_{003}) of NO_3-LDH, 0.83 nm, does not change after mixing with NBR matrix, but the peak is weak, indicative of disordering and no intercalation. When a polymer is unable to intercalate between the LDH layers, a phase-separated composite is obtained, which means that a poor interfacial interaction exists.[30] As can be seen from Figure 4 (peak c), the basal spacing (d_{003}) of SSS-LDH is shifted from 1.87 to 2.69 nm, indicative of partial intercalation and better interfacial interaction achieved. The opposite result is seen for the SDBS-LDH (Figure 4, peak d), in which the basal spacing (d_{003}) was decreased from 2.96 to 2.69 nm. During the curing of NBR-SL, polymerization and grafting reaction of SSS can enlarge the spacing and/or the polymer chain intercalated into the galleries. However, for the NBR-SDL, the coupling of adjacent polymer chain in the third step of vulcanization led to decrease in spacing, and therefore, different d_{003} spacing shifts were observed for the NBR/LDH compounds.

Morphological Structure of NBR/LDH Composites

The low-magnification SEM images shown in Figure 5 reveal the overview of frozen-cracked surface morphology of the three composites. It is apparent that the interfacial morphology between LDHs and NBR matrix follows different mechanisms in the three compounds. For NBR-L and NBR-SDL composites, LDH particles disperse nonuniformly in NBR and displays typical LDH aggregations. Additionally, it appears that the interfacial bonding of LDH–rubber matrix is not strong as some smooth holes and aggregates are presented in the fracture surface [Figure 5(A,C)]. This is possibly resulted from the poor compatibility between these two LDHs (NO_3-LDH and SDBS-LDH) and rubber matrix. For the NBR/SL composite, seen in Figure 5(B), it is apparent that the holes disappear and the layers disperse more uniformly with much smaller size in the NBR matrix. SEM observations are greatly in accordance with the XRD results, which demonstrate that the SSS is in favor of both interfacial interaction and dispersion.[40]

The conclusions made from the XRD patterns of the nanocomposites can be further established by analyzing the TEM micrographs of these materials. These micrographs for three nanocomposites are summarized in Figure 6. The TEM image clearly reveals very different nature of morphology due to different organic modification of LDHs. In case of NBR/LDH nanocomposite [Figure 6(A)], LDH particles are mostly clusters, whereas in NBR/SDL nanocomposite [Figure 6(C)], the proportion of clusters is decreased and intercalated fragments predominate. The best dispersion is visualized in NBR/SL nanocomposite [Figure 6(B)] system, in which almost no clusters were observed and LDH particle fragments are homogenously dispersed. This is due to the fact that interfacial interaction between polymer matrix and LDH differs after organic modification: SSS exhibits the strongest interaction due to the reactivity property, and the pure LDH aggregated because of poor hydrophobic property. Although XRD does not give any concrete information about the dispersion, the TEM images clearly demonstrate the

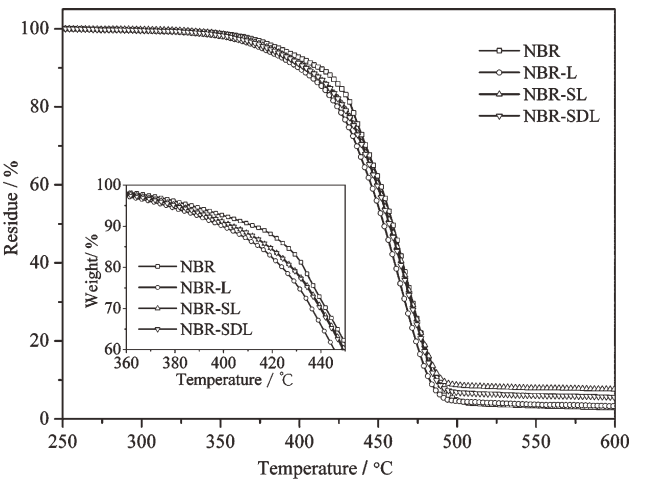

Figure 7. TGA traces obtained from NBR compounds.

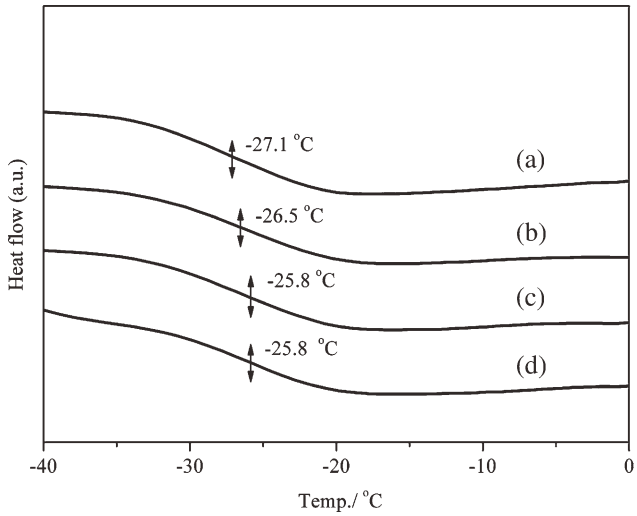

Figure 8. DSC curves obtained from (a) NBR, (b) NBR-L, (c) NBR-SL, and (d) NBR-SDL.

distribution morphology of three different LDHs in NBR matrix and also in accordance with SEM micrographs that showed the overview dispersion of LDHs particles. For instance, the NBR/LDH nanocomposite in Figure 6(A) displays LDH particles in the form of clusters, whereas the SEM displays macro-LDH aggregations.

Mechanical Properties

Mechanical properties testing were carried out to evaluate the improvement of the LDH-reinforced rubber. Table IV shows the results of unmodified and modified NBR/LDH composites. The SSS-LDH-modified NBR display remarkably higher improvement on tensile strength than NBR, NBR-L, and NBR-SDL. The hardness of NBR-SL is the highest among these compounds, which is in accordance with the conclusion provided in the work of Dluzneski.[34] However, the increase in tensile strength did not sacrifice much of the elongation at break. This is partially due to intercalation of the rubber matrix, which allows the fillers to interact more intensely with the polymer because of the polymerization and grafting reaction. The mechanical properties strongly testified that the SSS as a modifier and coagent in improving the interfacial interaction was successful.

TGA Analysis

TGA was used for studying the effect of LDHs on the thermal stability of the composites, and the results are shown in Figure 7. The $T_{5\%}$, $T_{10\%}$, and $T_{50\%}$ decrease with the addition of LDHs, especially when neat LDH was added. This is probably due to the degradation of the LDH.[41] It means that LDH does not improve the thermal stability of NBR. The amount of residue of NBR-SL is larger than what might be expected based on the LDH content and the rubber (the expected value is 4.5, 4.7, and 4.3% corresponding to NBR-L, NBR-SL, and NBR-SDL, respectively); it is possible that some charring of the polymer occurs and the residue consists of both carbonaceous char from the polymer along with LDH residue.[11] This is correlated to the highest char residue produced for SSS-LDH in Figure 2.

DSC Characteristics

The glass transition is an important thermal parameter that can be used to characterize polymers in the form of amorphous or semicrystalline materials. A variation of the glass transition of composites relative to the virgin polymer prepared under identical condition can provide evidence of possible specific interaction between the particles and the polymer matrix. In this study, an increase of glass transition temperature (T_g) was observed for all NBR composites as shown in Figure 8. The T_g of unmodified NBR-L composites is 0.6°C higher than that of pristine NBR, whereas T_gs of the NBR-SL and NBR-SDL are 1.3°C higher; this is caused by interactions between the inorganic fillers and the organic matrix.[42] As LDHs modified by SSS and SDBS, the LDH particles are dispersed in the NBR matrix first through organic modifiers, and then SSS is grafted or polymerized to form a new boundary, whereas the SDBS as a barrier interferes with free mobilization of the chain. The results suggest that new molecular interactions at the boundaries result from the presence of the SSS at the interface between the NBR and LDH layers.

CONCLUSION

Two different organic LDHs, SDBS-LDH without and SSS-LDH with organic modifier containing double bond, have been synthesized and added into NBR. NBR/LDH composites with different organically modified LDHs are successfully prepared to explore the effect of organic modifiers. Chemical bonding between organically modified LDHs and rubber matrix through SSS was built during vulcanization, which leads to improved interfacial strength of the cured compound. The tensile and shore A hardness test shows that NBR-SL gives better strength and hardness than that in NBR-SDL, which has two times higher tensile strength than cured pure rubber without significant loss of elongation. Furthermore, the intercalated structure of NBR/SL is also favorable of better mechanical properties. It can be concluded that the reactive double-bond-modified LDH would be greatly enhancing the interface interaction between NBR and LDH in peroxide curing process, resulting in composites with excellent properties that may be used in industry.

ACKNOWLEDGMENTS

The authors appreciate Dr. Cao, College of Chemistry and Chemical Engineering, Hunan University, Hunan, China, for obtaining the digital X-ray diffraction patterns.

REFERENCES

1. Nyambo, C.; Kandare, E.; Wilkie, C. A. *Polym. Degrad. Stab.* **2009,** *94*, 513.
2. Du, L. C.; Qu, B. J.; Zhang, M. *Polym. Degrad. Stab.* **2007,** *92*, 497.
3. Wang, Z. Y.; Han, E. H.; Ke, W. *Prog. Org. Coat.* **2005,** *53*, 29.
4. Ming, Z.; Peng, D.; Baojun, Q.; Aiguo, G. *J. Mater. Process. Technol.* **2008,** *208*, 342.
5. Chen, W.; Qu, B. J. *J. Mater. Chem.* **2004,** *14*, 1705.
6. Yamamoto, A.; Katamoto, T.; http://www.freepatentsonline.com/JP2004043701.html. 2004, JP 2004043701.

7. Cavani, F.; Trifiro, F.; Vaccari, A. *Catal. Today* **1991,** *11*, 173.
8. Xu, Z. P.; Braterman, P. S. *J. Phys. Chem. C* **2007,** *111*, 4021.
9. Morel-Desrosiers, N.; Pisson, J.; Israeli, Y.; Taviot, G. C.; Besse, J. P.; Morel, J. P. *J. Mater. Chem.* **2003,** *13*, 2582.
10. Manzi-Nshuti, C.; Wang, D. Y.; Hossenlopp, J. M.; Wilkie, C. A. *J. Mater. Chem.* **2008,** *18*, 3091.
11. Wang, L. J.; Su, S. P.; Chen, D.; Wilkie, C. A. *Polym. Degrad. Stab.* **2009,** *94*, 770.
12. Nyambo, C.; Wang, D.; Wilkie, C. A. *Polym. Adv. Technol.* **2009,** *20*, 332.
13. Zammarano, M.; Bellayer, S.; Gilman, J. W.; Franceschi, M.; Beyer, F. L.; Harris, R. H.; Meriani, S. *Polymer* **2006,** *47*, 652.
14. Chen, G. M. *J. Nanosci. Nanotechnol.* **2006,** *6*, 1155.
15. Yong-Zhong, B.; Zhi-Ming, H.; Zhi-Xue, W. *J. Appl. Polym. Sci.* **2006,** *102*, 1471.
16. Tseng, C. H.; Hsueh, H. B.; Chen, C. Y. *Compos. Sci. Technol.* **2007,** *67*, 2350.
17. Hsueh, H. B.; Chen, C. Y. *Polymer* **2003,** *44*, 5275.
18. Costa, F. R.; Wagenknecht, U.; Heinrich, G. *Polym. Degrad. Stab.* **2007,** *92*, 1813.
19. Baojun, Q.; Qiu, L.; Wei, C. *Polymer* **2006,** *47*, 922.
20. Costa, F. R.; Abdel-Goad, M.; Wagenknecht, U.; Heinrich, G. *Polymer* **2005,** *46*, 4447.
21. Du, L. C.; Qu, B. J. *Chin. J. Chem.* **2006,** *24*, 1342.
22. Kuila, T.; Acharya, H.; Srivastava, S. K.; Bhowmick, A. K. *J. Appl. Polym. Sci.* **2007,** *104*, 1845.
23. Kuila, T.; Acharya, H.; Srivastava, S. K.; Bhowmick, A. K. *J. Appl. Polym. Sci.* **2008,** *108*, 1329.
24. Kuila, T.; Acharya, H.; Srivastava, S. K.; Bhowmick, A. K. *Polym. Compos.* **2009,** *30*, 497.
25. Kuila, T.; Srivastava, S. K.; Bhowmick, A. K. *J. Appl. Polym. Sci.* **2009,** *111*, 635.
26. Kuila, T.; Srivastava, S. K.; Bhowmick, A. K. *Polym. Eng. Sci.* **2009,** *49*, 585.
27. Acharya, H.; Srivastava, S. K.; Bhowmick, A. K. *Compos. Sci. Technol.* **2007,** *67*, 2807.
28. Pradhan, S.; Costa, F. R.; Wagenknecht, U.; Jehnichen, D.; Bhowmick, A. K.; Heinrich, G. *Eur. Polym. J.* **2008,** *44*, 3122.
29. Das, A.; Costa, F. R.; Wagenknecht, U.; Heinrich, G. *Eur. Polym. J.* **2008,** *44*, 3456.
30. Abdullah, M. A. A.; Ahmad, M. B.; Yunus, W.; Rahman, M. Z. A.; Hussein, M. Z.; Dahalan, K. Z. M. *Solid State Sci. Technol.* **2007,** *909*, 228.
31. Geng, H.; Zedong, L.; Dan, C.; Shengpei, S. *Fine Chem Intermed.* **2009,** *39*, 52.
32. Meyn, M.; Benecke, K.; Lagally, G. *Inorg. Chem.* **1990,** *29*, 5201.
33. Mark, H. F.; Bikales, N.; Overberger, C. G.; Menges, G.; Kroschwitz, J. I.Encyclopedia of Polymer Science and Engineering;Wiley:New York, **1990.**
34. Dluzneski, P. R. *Rubber World* **2001,** *224*, 34.
35. Henning, S. K.; Boye, W. M. *Rubber World* **2009,** *240*, 31.
36. Henning, S. K.; Sartomer, R. C. *Rubber World* **2006,** *233*, 28.
37. Martinez-Gallegos, S.; Herrero, M.; Barriga, C.; Labajos, F. M.; Rives, V. *Appl. Clay Sci.* **2009,** *45*, 44.
38. Hwang, W. G.; Wei, K. H.; Wu, C. M. *Polym. Eng. Sci.* **2004,** *44*, 2117.
39. Wang, L. J.; Su, S. P.; Chen, D.; Wilkie, C. A. *Polym. Degrad. Stab.* **2009,** *94*, 1110.
40. Jia, Q. X.; Wu, Y. P.; Wang, Y. Q.; Lu, M.; Zhang, L. Q. *Compos. Sci. Technol.* **2008,** *68*, 1050.
41. Manzi-Nshuti, C.; Chen, D.; Su, S. P.; Wilkie, C. A. *Polym. Degrad. Stab.* **2009,** *94*, 1290.
42. Yehia, A. A.; Mansour, A. A.; Stoll, B. *J. Therm. Anal.* **1997,** *48*, 1299.